HAL
open science

Experimental demonstration of nonbilocal quantum correlations

Dylan Saunders, Adam J. Bennet, Cyril Branciard, Geoff J. Pryde

To cite this version:

Dylan Saunders, Adam J. Bennet, Cyril Branciard, Geoff J. Pryde. Experimental demonstration of nonbilocal quantum correlations. Science Advances , 2017, 3 (4), pp.1602743. 10.1126/sciadv.1602743 . hal-01632382

HAL Id: hal-01632382

https://hal.science/hal-01632382v1

Submitted on 26 May 2021

HAL is a multi-disciplinary open access archive for the deposit and dissemination of scientific research documents, whether they are published or not. The documents may come from teaching and research institutions in France or abroad, or from public or private research centers.

L'archive ouverte pluridisciplinaire **HAL**, est destinée au dépôt et à la diffusion de documents scientifiques de niveau recherche, publiés ou non, émanant des établissements d'enseignement et de recherche français ou étrangers, des laboratoires publics ou privés.

QUANTUM NETWORKS

Experimental demonstration of nonbilocal quantum correlations

Dylan J. Saunders,[1,2]* Adam J. Bennet,[1] Cyril Branciard,[3] Geoff J. Pryde[1]

2017 © The Authors, some rights reserved; exclusive licensee American Association for the Advancement of Science. Distributed under a Creative Commons Attribution NonCommercial License 4.0 (CC BY-NC).

Quantum mechanics admits correlations that cannot be explained by local realistic models. The most studied models are the standard local hidden variable models, which satisfy the well-known Bell inequalities. To date, most works have focused on bipartite entangled systems. We consider correlations between three parties connected via two independent entangled states. We investigate the new type of so-called "bilocal" models, which correspondingly involve two independent hidden variables. These models describe scenarios that naturally arise in quantum networks, where several independent entanglement sources are used. Using photonic qubits, we build such a linear three-node quantum network and demonstrate nonbilocal correlations by violating a Bell-like inequality tailored for bilocal models. Furthermore, we show that the demonstration of nonbilocality is more noise-tolerant than that of standard Bell nonlocality in our three-party quantum network.

INTRODUCTION

Bell's theorem (*1*) resolved the long-standing Einstein-Podolsky-Rosen debate (*2*) by demonstrating that no local realistic theory can reproduce the correlations observed when performing appropriate measurements on some entangled quantum states—so-called (Bell) nonlocal correlations (*3*). Entanglement now finds applications as a resource in many quantum information and communication protocols [for example, see the studies by Ekert (*4*) and Bennett *et al.* (*5*)]. In most fundamental or applied experiments to date, the entangled systems come directly from a single source. However, sometimes, more than one source of entanglement is used, such as in protocols that rely on entanglement swapping (*6*) to generate entanglement between two parties at the ends of a chain (although they share no common history). Because the entanglement swapping results in a bipartite entangled state, one may examine this "network" scenario by considering only the nonlocality of the correlations between the measurement outcomes at the terminal nodes. An "event-ready" Bell test (*6*), heralded on success signals from all intermediate nodes, would then aim to disprove a local theory that is based on a single local hidden variable (LHV) model. However, such a test ignores properties of the intermediate channel, such as the fact that the multiple sources of entanglement may be independent of each other. This raises an important fundamental question: How does source independence affect the notion of nonlocality?

To address this question, a new type of LHV model was recently considered, where the independence properties of the different sources in an experimental setup are also imposed at the level of the hidden variables (*7*, *8*). The simplest nontrival quantum network to analyze this new type of model is a three-node linear network, as depicted in Fig. 1. In such a network, two independent entanglement sources connect the three nodes, Alice, Bob, and Charlie; the corresponding model, which involves two independent LHVs, is termed "bilocal." Just like standard LHV models satisfy Bell inequalities, it was shown that bilocal models impose constraints on the corresponding correlations in the form of (nonlinear) Bell-like inequalities—so-called "bilocal inequalities"—which can be violated quantum mechanically (*7*, *8*).

[1]Centre for Quantum Dynamics and Centre for Quantum Computation and Communication Technology, Griffith University, Brisbane, Queensland 4111, Australia. [2]Clarendon Laboratory, University of Oxford, Parks Road, Oxford OX1 3PU, U.K. [3]Institut Néel, CNRS and Université Grenoble Alpes, 38042 Grenoble Cedex 9, France.
*Corresponding author. Email: dylan.saunders@physics.ox.ac.uk

One advantage of considering bilocal models is that one may demonstrate nonbilocality in situations where no nonlocality could be obtained. For example, in an entanglement swapping experiment that generates a two-qubit Werner state between Alice and Charlie of the form $\rho w(v) = v|\psi\rangle\langle\psi| + (1-v)\frac{\mathbb{1}}{4}$ (where $|\psi\rangle$ is a maximally entangled state and $\frac{\mathbb{1}}{4}$ is the maximally mixed state), a visibility $v > 1/\sqrt{2}$ is required to violate the commonly used Clauser-Horne-Shimony-Holt (CHSH) Bell inequality (*9*), whereas bilocal inequalities can detect nonbilocality for any $v > 1/2$ (*7*, *8*); thus, one can certify the absence of a bilocal LHV model under more noise compared to a Bell local model.

The aim of the present work is to experimentally investigate quantum nonbilocal correlations. We implement the scenarios of Fig. 1 in a photonic setup. In our experiment, the entangled photon pairs originate from two nonlinear crystals pumped separately, although by the same laser beam. To enhance the independence of the two sources, we actively destroy any coherence in the pump beam between the two crystals. We test two different bilocal inequalities and find violations that allow us to disprove bilocal models for the quantum correlations observed.

Local versus bilocal models

The differences between testing locality and bilocality on a three-node quantum network are highlighted in Fig. 1. Let us first introduce a standard LHV three-party model: Consider a tripartite probability distribution of the form

$$P(a,b,c|x,y,z) = \int d\lambda\, \rho(\lambda) P(a|x,\lambda) P(b|y,\lambda) P(c|z,\lambda) \qquad (1)$$

where Alice, Bob, and Charlie have measurement inputs x, y, z and measurement outputs a, b, c, respectively, and the LHV λ with the distribution $\rho(\lambda)$ can be understood as describing the joint state of the three systems. $P(a|x,\lambda)$, $P(b|y,\lambda)$, and $P(c|z,\lambda)$ are the local probabilities for each separate outcome, given λ. A probability distribution $P(a,b,c|x,y,z)$ of the form of Eq. 1 is said to be (Bell) local; one that cannot be expressed in that form is called (Bell) nonlocal (*3*).

In a practical experiment, where the abovementioned tripartite probability distribution is obtained by measuring some physical systems—for example, particles—it is natural to assume that the LHV λ originates from the source that prepares and sends those

Downloaded from http://advances.sciencemag.org/ on May 25, 2021

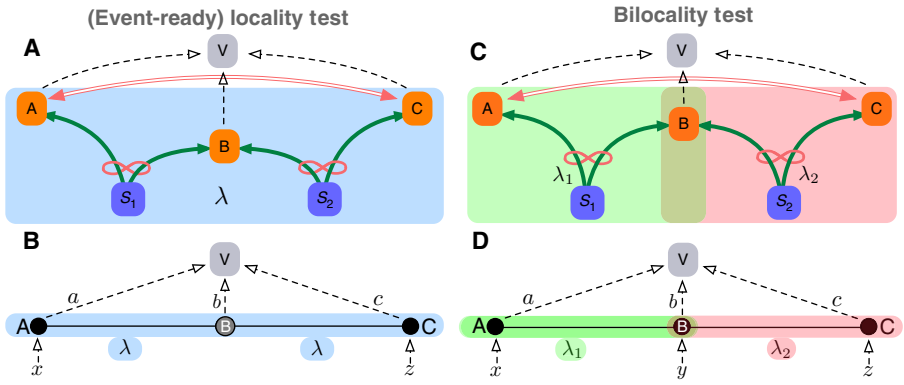

Fig. 1. Quantum network tests of locality and bilocality. Here we show an event-ready Bell test (**A** and **B**) and a test of bilocality (**C** and **D**) on a three-node network. (A) and (C) conceptually show the experimental arrangement involving the entangled photon pairs (green arrows) emitted from two independent sources (S_1 and S_2), the three nodes [Alice (A), Bob (B), and Charlie (C)], and a referee, Victor (V), who computes and analyzes the correlations between the inputs [measurement settings *x*, (*y*,) *z*] and outputs (measurement results *a*, *b*, *c*) of A, B, and C sent to him via classical communication channels (dashed arrows). The diagrams also show the regions of influence of the LHVs in the two models under consideration, λ (blue shading) for the (Bell) locality case or λ_1 (green shading) and λ_2 (salmon shading) for bilocality. The pink double arrow represents the quantum correlations between the terminal nodes in each case. The physical arrangement is such that Bob's measurement device has two input ports (incoming channels, green arrows), one from each source (S_1 and S_2). In the simplest event-ready implementation (A and B), Bob's measurement result *b* is a binary variable that heralds a trial of a Bell test between Alice and Charlie, when Bob's (fixed) Bell state measurement (BSM) successfully projects his two incoming systems onto, for example, the singlet state (*6*). In (C) and (D), on the other hand, *b* may be composed of more than one bit (corresponding to the result of a more informative joint measurement by Bob) and is taken into account in the test of a bilocal inequality. (B) and (D) highlight the different network architecture of the two tests, including the nodes and connections (solid lines), the input measurement settings (*x*, *y*, *z*), and the measurement results (*a*, *b*, *c*).

systems. However, for our three-node quantum network of Fig. 1, there are two independent sources of entangled particles—S_1 and S_2. It is then natural to consider two LHVs, λ_1 and λ_2, one attached to each source, and write

$$P(a,b,c|x,y,z) = \int d\lambda_1\, d\lambda_2\, \rho(\lambda_1\lambda_2) P(a|x,\lambda_1) P(b|y,\lambda_1,\lambda_2) P(c|z,\lambda_2) \tag{2}$$

Here, the local probabilities of each party are conditioned only on the LHV(s) attached to the source(s) from which they receive the particles: λ_1 for Alice, λ_2 for Charlie, and both λ_1 and λ_2 for Bob, at the intermediate node. So far, the correlations producible by the local decompositions in Eqs. 1 and 2 are equivalent. For example, the joint distribution of the two LHVs $\rho(\lambda_1, \lambda_2)$ could be nonzero only when $\lambda_1 = \lambda_2 = \lambda$ (*7*). However, we shall now introduce the critical bilocality assumption, based on the physical arrangement of our quantum network: The independence of the two sources S_1 and S_2 carries over to the LHVs λ_1 and λ_2. That is, their joint distribution $\rho(\lambda_1, \lambda_2)$ must factorize

$$\rho(\lambda_1,\lambda_2) = \rho(\lambda_1)\rho(\lambda_2) \tag{3}$$

Probability distributions $P(a, b, c|x, y, z)$ that can be expressed as in Eq. 2, with $\rho(\lambda_1, \lambda_2)$ satisfying Eq. 3, are said to be "bilocal;" those that cannot be expressed as such are termed "nonbilocal" (*7*, *8*).

Demonstrating nonbilocality

The decomposition of Eq. 2, together with Eq. 3, imposes certain restrictions on the correlations that can be produced by bilocal models. Note that any bilocal model is in particular Bell local, so that it must satisfy all Bell inequalities; any violation of a Bell inequality is already a demonstration of nonbilocality. However, it is also possible to derive stronger constraints for bilocal models, which specifically make use of the independence condition of Eq. 3. In the study by Branciard *et al.* (*8*), different bilocal inequalities were obtained, of the general form

$$\mathcal{B} := \sqrt{|I|} + \sqrt{|J|} \leq 1 \tag{4}$$

where *I* and *J* are linear combinations of the observed probabilities $P(a, b, c|x, y, z)$ (see Methods for details). A violation of such an inequality, that is, a $\mathcal{B}$ value greater than 1, is a proof of nonbilocality, as it rules out any possible bilocal model—in a similar way that a CHSH value, $\mathcal{B}_{\mathrm{CHSH}}$, greater than 2 disproves any Bell local model (see the Supplementary Materials) (*9*).

The bilocal inequalities described above apply to scenarios where Alice and Charlie have binary inputs and outputs. As for Bob, we consider two cases that are of particular experimental relevance. In the first case, he has a single fixed input (measurement setting) and four possible outputs (measurement results); following the notations of Branciard *et al.* (*8*), we shall label this case "*14*" and write the corresponding inequality as $\mathcal{B}_{14} \leq 1$. In the second case, Bob still has a fixed input, but he now has three possible outputs; we shall label this case "*13*" and write $\mathcal{B}_{13} \leq 1$. As discussed below, these two cases will correspond in the experiment to a full and a partial BSM implemented by Bob, respectively.

RESULTS

To test the two bilocal inequalities $\mathcal{B}_{14}, \mathcal{B}_{13} \leq 1$, we realized a photonic implementation of an entanglement swapping type of experiment [for example, see the study by Pan *et al.* (*10*)] that implements the three-node quantum network of Fig. 1. Two "sandwich" type 1 spontaneous parametric downconversion (SPDC) sources (*11*) supplied the entangled photonic links between the nodes (see Fig. 2). To justify that the bilocality assumption is reasonable, one should ideally have truly independent sources. In our case, we used two separate nonlinear

Downloaded from http://advances.sciencemag.org/ on May 25, 2021

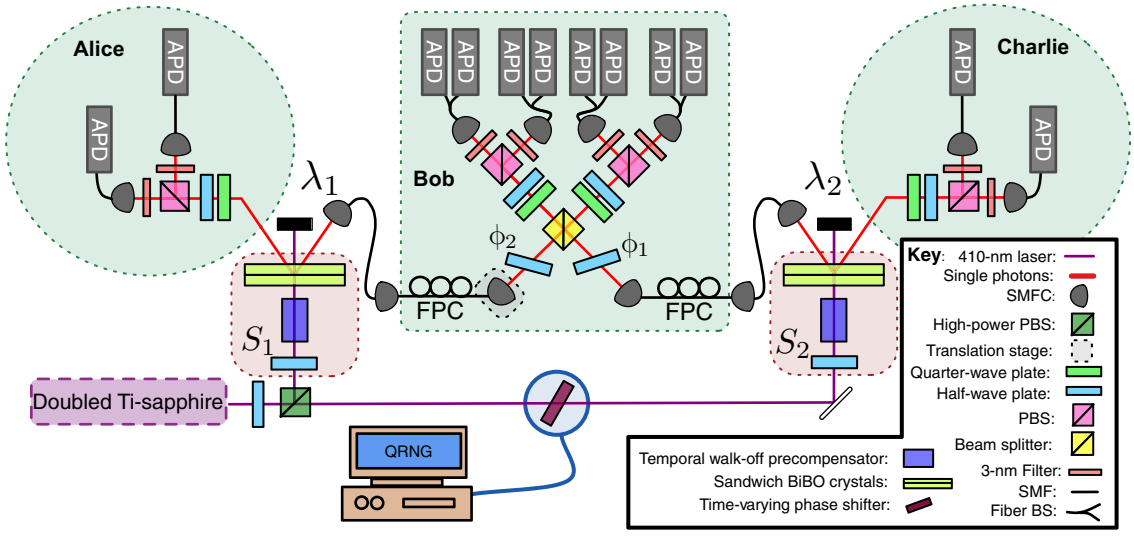

Fig. 2. Experimental setup to test bilocality in a three-node quantum network. The nodes—Alice, Bob, and Charlie—are highlighted in green, and the entanglement sources connecting them—$S_1$and S_2—are highlighted in red. Both entanglement sources [sandwich bismuth triborate (BiBO) crystals and temporal walk-off precompensators (*11*)] are pumped by a mode-locked, 410-nm, 80-MHz frequency–doubled titanium-sapphire oscillator. To substantiate the assumption that the LHVs λ_1 and λ_2 attached to the two sources are independent, we erased any coherence in the pump beam between S_1 and S_2 via a time-varying phase shifter (TVPS) set using a quantum random number generator (QRNG) (see the Results and the Supplementary Materials for details). Alice and Charlie implement their measurements (with settings *x*, *z* and outputs *a*, *c*) using polarization optics: quarter–wave plates, half–wave plates, polarizing beam splitters (PBSs), single-mode fibers (SMFs), and single-mode fiber couplers (SMFCs). Bob implements his BSM using a 50:50 beam splitter (BS) and polarization optics, which has two input ports (incoming channels), one from each entanglement source. Bob ensures that he implements the correct BSM (that is, he projects onto the desired Bell state in the simulated full BSM) (see Results) by implementing single-qubit unitaries using a fiber polarization controller (FPC) and phase gates (ϕ_1 and ϕ_2, tilted half–wave plates), with each combination corresponding to one of the simulated measurement outputs, *b*. Bob also implements pseudo–number-resolving detectors on each of his four output ports when implementing the partial BSM (see Results), using a fiber 50:50 BS (fiber BS) to split each output port into two bucket avalanche photon detectors (APDs). We observe four-photon coincidence events—one click for Alice and Charlie and two clicks for Bob—on the APDs using a field programmable gate array, with a coincidence window of 3 ns to signify successful operation of our quantum network and to calculate all probabilities $P(a, b, c|x, y, z)$. Further experimental details are given in the Supplementary Materials.

crystals to realize the parametric downconversion; however, the two crystals were pumped by a strong beam originating from the same laser. To increase the degree of independence between the two sources, we installed a TVPS in the pump beam before the source S_2. The TVPS comprised a rotatable optical flat connected to an automated stage and a remote quantum random number generator (*12*), adding a genuinely random phase offset between sources S_1 and S_2 on each trial of the experiment and thus destroying any quantum coherence (see the Supplementary Materials for details).

At the central node, Bob implements an entangling BSM (*13*) to essentially fuse the two sources of entanglement S_1 and S_2 via entanglement swapping (*6*). Using linear optics only, it is impossible to construct an ideal BSM device that reliably discriminates between all four Bell states, which would be necessary for deterministic entanglement swapping (*14*). However, it is possible to experimentally simulate the statistics of an ideal BSM. We construct such a BSM device that projects onto one of the four Bell states. We then implement local unitaries to project separately, in different experimental runs, onto the three remaining states and combine the statistics at the end of the experiment to mimic a universal BSM device. In this case, Bob's implemented measurement device has four input settings (one for each of the canonical Bell states, $|\Phi^+\rangle$, $|\Phi^-\rangle$, $|\Psi^+\rangle$, and $|\Psi^-\rangle$) and one bit of output (indicating successful projection onto the relevant state)—such that on each run of the experiment, we only project onto a single Bell state. After recombining the statistics at the end of the experiment, Bob has simulated an ideal BSM device with a single input setting (corresponding to precisely performing a BSM) and four possible measurement results (outputs b), one corresponding to each of the four Bell states. It is precisely in this one-input/four-output scenario that one can test the $\mathcal{B}_{14} \leq 1$ bilocal inequality introduced previously. Conveniently, it is also possible using linear optics to construct a partial BSM device that projectively resolves two of the four Bell states (for example, $|\Phi^+\rangle$ and $|\Phi^-\rangle$), accompanied by a third projection that groups the remaining two Bell states (for example, $|\Psi^\pm\rangle$) into a single outcome (*15*)—a single-input, three-output measurement that allows one to test the $\mathcal{B}_{13} \leq 1$ bilocal inequality. As for Alice and Charlie, as mentioned above, they should have binary inputs (measurement settings) and outputs (measurement results) to test these two inequalities. We implemented projective measurements of the observables $\hat{A}_x$ and $\hat{C}_z$ (depending on the inputs $x, z = 0, 1$) defined as $\hat{A}_0 = \hat{C}_0 = (\hat{\sigma}_z + \hat{\sigma}_x)/\sqrt{2}$ (using the corresponding half–wave plate setting $\theta_0 = 11.25°$) and $\hat{A}_1 = \hat{C}_1 = (\hat{\sigma}_z - \hat{\sigma}_x)/\sqrt{2}$ ($\theta_1 = -11.25°$) in the *14* case (where $\hat{\sigma}_{z,x}$ are the standard Pauli matrices) and as $\hat{A}_0 = \hat{C}_0 = (\sqrt{2}\hat{\sigma}_z + \hat{\sigma}_x)/\sqrt{3}$ ($\theta_0 \approx 8.82°$) and $\hat{A}_1 = \hat{C}_1 = (\sqrt{2}\hat{\sigma}_z - \hat{\sigma}_x)/\sqrt{3}$ ($\theta_1 \approx -8.82°$) in the *13* case, which, in principle, provide the optimal violations of the two inequalities (*8*).

Each entanglement source S_i ($i = 1, 2$) ideally produces a pure Bell state. However, because of minor experimental imperfections, the produced states were close to Werner states (as described in the Introduction) with visibility $v_i \gtrsim 0.94$ [determined via quantum state tomography (*16*)] for both sources for all implementations of Bob's BSM. The fidelity of the BSM was maximized using single-mode fibers, narrowband frequency filters (~3-nm full width at half maximum), and a high-precision translation stage, affording subcoherence length timing

Downloaded from http://advances.sciencemag.org/ on May 25, 2021

resolution and ensuring high-quality Hong-Ou-Mandel (HOM) interference. We measured a resultant HOM visibility of $v_{1,2}^{\mathrm{BSM}} = (85{\pm}5)\%$ when Bob implemented the *14*-BSM and $v_{1,2}^{\mathrm{BSM}} = (91{\pm}3)\%$ for Bob's *13*-BSM. The visibility of the closest Werner state to the resultant entangled state at Alice's and Charlie's terminal nodes (conditioned on Bob's BSM result) was estimated using quantum state tomography, yielding $v_{14} \approx 0.78$ and $v_{13} \approx 0.85$, respectively—in agreement with the product of the visibility of each entangled source and the BSM visibility, as expected.

To further verify that our network was producing Werner-like states, we compared the measured CHSH inequality with the inferred entanglement visibilities. We tested the CHSH inequality $\mathcal{B}_{\mathrm{CHSH}} \leq 2$ (see the Supplementary Materials) (*9*) on the resultant state of Alice and Charlie after successful entanglement swapping, a standard [event-ready (*6*)] test of Bell locality. We recorded $\mathcal{B}_{\mathrm{CHSH}}^{14} = 2.22 \pm 0.06$ and $\mathcal{B}_{\mathrm{CHSH}}^{13} = 2.41 \pm 0.05$, agreeing with the measured v's above, and both with clear violations of the local bound. Next, the bilocal inequalities of Eq. 4, for both the full (case "*14*") and partial (case "*13*") BSMs, were tested in our network, with clear violations in both cases: $\mathcal{B}_{14} = 1.25 \pm 0.04 > 1$ and $\mathcal{B}_{13} = 1.17 \pm 0.02 > 1$ (see the Supplementary Materials for further details). To explore the noise robustness of our locality and bilocality tests, we added various amounts of white noise to our experimental data (see Fig. 3). We implemented this by swapping the labels on Alice's measurement outcomes on selected experimental runs, mimicking the effect of white noise by washing out the correlations (see Methods). This experimentally verified the prediction that in the presence of noise, there exists a region where nonbilocal correlations can be observed but nonlocal correlations cannot (*7*, *8*).

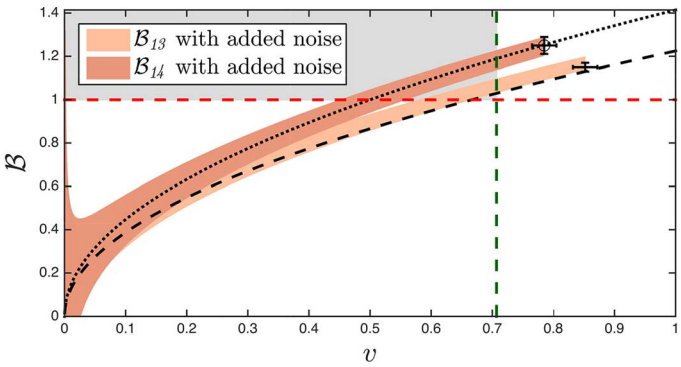

Fig. 3. Evidence of noise-tolerant nonbilocality. We measured bilocality parameters and estimated the corresponding values of visibility v obtained for the best quality of our network (the ○ data point corresponds to $\mathcal{B}_{14}$ and the other one corresponds to $\mathcal{B}_{13}$). The error bars for $\mathcal{B}$ arise from Poissonian statistics, whereas the error on v is calculated using the product of the source visibility v_i and the measured HOM dip visibility $v_{1,2}^{\mathrm{BSM}}$ and agrees with the measured $\mathcal{B}_{\mathrm{CHSH}}$ (see the main text and the Supplementary Materials for details). To test the noise tolerance of nonbilocal correlations, we introduce noise in our data by randomly "flipping" trials of Alice's measurement (see Methods), allowing us to predict the performance of our network to added white noise by simulating Werner states with $v_{14} \approx 0.78$ and $v_{13} \approx 0.85$, the maximum entanglement visibilities of our networks. The orange-shaded areas show the expected performance of our network under added noise to ±1 SD. The dashed (dotted) lines are the expected values for $\mathcal{B}_{14}(v) = \sqrt{2v}$ and $\mathcal{B}_{13}(v) = \sqrt{3v/2}$ (*8*). Both sets of experimental values for $\mathcal{B}_{14}(v)$ and $\mathcal{B}_{13}(v)$ (orange-shaded areas) occupy the region that is nonbilocal ($\mathcal{B} > 1$; above the red dashed line) and will not violate the CHSH inequality, for $v \leq 1/\sqrt{2}$ (left of the green dashed line) (gray-shaded region). Note that in our case with binary inputs and outputs for Alice and Charlie and a fixed measurement setting for Bob, CHSH (with its symmetries) is the only relevant Bell inequality (*39*, *40*). This provides evidence for the higher noise tolerance of nonbilocal correlations compared to Bell nonlocal correlations.

DISCUSSION

We have thus experimentally demonstrated the violation of two Bell-like inequalities tailored for quantum networks with independent entanglement sources and verified that those inequalities can be violated at added noise levels for which a CHSH inequality cannot. As with quantum (EPR-) steering (*17*), for example, the addition of an extra assumption (here, source independence) relaxes the stringent intolerance to noise of nonlocality demonstrations.

Our violation of bilocal inequalities shows, in principle, that no bilocal model can explain the correlations we observed. However, we acknowledge that, like most Bell tests until very recently (*18*–*20*), our experiment is subject to some loopholes. In addition to the issue of space-like separation and the detection loophole (*21*), the specificity of the bilocality assumption opens a new "source independence loophole" when the entanglement sources are not guaranteed to be fully independent. In our experiment, we enhanced the source independence by erasing the quantum coherence between the pump beams of our two separate SPDC sources. Nevertheless, the bilocality violations we observed could still, in principle, be explained by some hidden mechanism that would correlate the two sources (and the two LHVs λ_1, λ_2 attached to them in a bilocal model), for instance, via the shared pump beam. To be able to draw more satisfying conclusions with regard to nonbilocality, the next step will be to realize a similar experiment with "truly independent" sources [following in the footsteps of Kaltenbaek *et al.* (*22*) and Erven *et al.* (*23*)]—but keeping in mind that just like a Bell test can never rule out a superdeterministic explanation (*24*), it is impossible to guarantee that two separate sources are genuinely independent, as they could have been correlated at the birth of the universe.

The bilocality assumption, as well as its extension to "*N*-locality" in more complex scenarios involving *N*-independent sources, provides a natural framework to explore and characterize quantum correlations in multisource, multiparty networks (*7*, *8*). "*N*-local inequalities" have been derived in the line of Bell and bilocal inequalities (*25*–*33*), which could be tested in possible extensions of the present experiment and in future larger quantum networks. An interesting question is whether the violation of these inequalities could be directly exploited and could allow for useful applications in quantum information processing—similar to the demonstration of Bell nonlocality or quantum steering which can, for example, be used to certify the security of quantum key distribution, or the privacy of randomness generation, in a device-independent way (*34*–*37*). We note that, contrary to the event-ready Bell test, the violation of the bilocal inequalities tested here does not by itself certify that Bob must have performed an entangling measurement and that Alice and Charlie end up sharing an entangled state (a counterexample is presented in the Supplementary Materials); thus, it is not sufficient for information processing protocols that require such a certification. However, we expect other possible applications to be discovered, which will fully harness the non–*N* locality of quantum correlations, for instance, in cases where nonlocality cannot be demonstrated. The problem of characterizing and demonstrating non–*N*-local correlations will become more and more crucial as future quantum networks continue to grow in size and complexity.

Downloaded from http://advances.sciencemag.org/ on May 25, 2021

Note Added. During the preparation of the paper, we became aware of an independent experimental study of nonbilocality (*38*).

METHODS

Bilocal inequalities

The quantities I and J in the bilocal inequalities $\mathcal{B} := \sqrt{|I|} + \sqrt{|J|} \leq 1$ (Eq. 4) that we tested in our experiment were defined from the observed probabilities $P(a, b, c|x, z)$ as follows. [Because we consider cases where Bob has a single fixed measurement setting y, we can ignore it when writing $P(a, b, c|x, z)$.]

Let us start with the full BSM, with four possible outcomes—the case labeled *14*. Here, Bob's output consists of two bits, $b = b^0b^1$. Using some of the notations and forms introduced by Branciard *et al.* (*8*), we first define, for $j = 0$ and 1, the tripartite correlators (expectation values)

$$\langle A_x B^j C_z \rangle_{P_{14}} := \sum_{a,b^0,b^1,c} (-1)^{a+b^j+c} P_{14}(a, b^0b^1, c|x, z) \tag{5}$$

where the sum is over all outputs a, b^0, b^1, $c = 0$, 1 of the three parties. These correlators, for the various values of x, $z = 0$, 1, then sum together in the following way to define I_{14} and J_{14} as

$$I_{14} := \frac{1}{4}\sum_{x,z} \langle A_x B^0 C_z \rangle_{P_{14}}, \quad J_{14} := \frac{1}{4}\sum_{x,z} (-1)^{x+z} \langle A_x B^1 C_z \rangle_{P_{14}} \tag{6}$$

The case of a partial three-outcome BSM, labeled *13*, is slightly complicated by the asymmetry in the partial BSM. Here, we denote Bob's three possible outcomes as $b = b^0b^1 = 00$, 01, {10 or 11}. The tripartite correlators are defined as

$$\langle A_x B^0 C_z \rangle_{P_{13}} := \sum_{a,c} (-1)^{a+c} [P_{13}(a, 00, c|x, z) + P_{13}(a, 01, c|x, z) - P_{13}(a, \{10 \text{ or } 11\}, c|x, z)] \tag{7}$$

and, restricting to the case where Bob gets one of the first two outcomes (that is, $b^0 = 0$)

$$\langle A_x B^1 C_z \rangle_{P_{13}, b^0=0} := \sum_{a,c} (-1)^{a+c} [P_{13}(a, 00, c|x, z) - P_{13}(a, 01, c|x, z)] \tag{8}$$

Similarly as before, these correlators then sum together to now define

$$I_{13} := \frac{1}{4}\sum_{x,z} \langle A_x B^0 C_z \rangle_{P_{13}}, \quad J_{13} := \frac{1}{4}\sum_{x,z} (-1)^{x+z} \langle A_x B^1 C_z \rangle_{P_{13}, b^0=0} \tag{9}$$

We provide in the Supplementary Materials all the probabilities $P(a, b, c|\, x, y)$ measured in both our *14* and *13* tests, which allowed us to compute our experimental values for I, J, and $\mathcal{B} := \sqrt{|I|} + \sqrt{|J|}$.

Adding noise to our network

To investigate the noise tolerance properties of testing different local and bilocal models in our quantum network, we added white noise to our measured correlations. Ideally, the joint state shared between Alice and Charlie (outer nodes) after entanglement swapping would be one of the four Bell states. However, because of experimental noise, the states produced can instead be approximated by a Werner state of the form

$$\rho w(v) = v|\psi\rangle\langle\psi| + (1 - v)\frac{\mathbb{1}}{4} \tag{10}$$

where $|\psi\rangle$ is the resulting shared Bell state after the swapping operation and $\frac{\mathbb{1}}{4}$ is the maximally mixed two-qubit state. In our experiment, the state W had visibilities of $v_{14} \approx 0.78$ and $v_{13} \approx 0.85$ before introducing further white noise; the values of v in the *14* and *13* cases mainly differ because of the differences in Bob's BSM visibility between runs. This agrees with the source visibilities determined using quantum state tomography and with the visibility of the BSM determined by measuring a heralded HOM dip visibility, by scanning the automated delay stage in Bob's BSM apparatus. This also agrees with the measured CHSH parameter values for our network.

To add further noise, our procedure was inspired by the effect of white noise on the observed statistics. We flipped Alice's measurements with probability $p = (1 - v_{\text{added}}/2)$ to simulate adding further noise with visibility v_{added}, ending up with a global visibility $v = v_{14/13}\, v_{\text{added}}$ for the state of Eq. 10. This mirrors the effect of a depolarizing channel for our polarization-encoded qubits, allowing us to vary the value of v for the Werner states produced in our network, up to the limit of $v \leq v_{14/13}$.

SUPPLEMENTARY MATERIALS

Supplementary material for this article is available at http://advances.sciencemag.org/cgi/content/full/3/4/e1602743/DC1

Characterization of the TVPS

Photon counting and experimental details

Experimental violation of the bilocal inequalities

Experimental violation of the CHSH inequality

Our bilocal inequalities violations are not device-independent certifications of A-C entanglement: Counterexample

table S1. Measured probabilities $P_{14}(a, b, c|x, z)$ and correlators $\langle A_x B^j C_z \rangle_{P_{14}}$ in our test of the $\mathcal{B}_{14} \leq 1$ bilocal inequality.

table S2. Measured probabilities $P_{13}(a, b, c|x, z)$ and correlators $\langle A_x B^j C_z \rangle_{P_{13}}$ in our test of the $\mathcal{B}_{13} \leq 1$ bilocal inequality.

table S3. Observed violations of the bilocal inequalities $\mathcal{B} := \sqrt{|I|} + \sqrt{|J|} \leq 1$.

REFERENCES AND NOTES

1. J. S. Bell, On the Einstein Podolsky Rosen paradox. *Physics* **1**, 195–200 (1964).
2. A. Einstein, B. Podolsky, N. Rosen, Can quantum-mechanical description of physical reality be considered complete? *Phys. Rev. Lett.* **47**, 777–780 (1935).
3. N. Brunner, D. Cavalcanti, S. Pironio, V. Scarani, S. Wehner, Bell nonlocality. *Rev. Mod. Phys.* **86**, 419–478 (2014).
4. A. K. Ekert, Quantum cryptography based on Bell's theorem. *Phys. Rev. Lett.* **67**, 661–663 (1991).
5. C. H. Bennett, G. Brassard, C. Crépeau, R. Jozsa, A. Peres, W. K. Wootters, Teleporting an unknown quantum state via dual classical and Einstein-Podolsky-Rosen channels. *Phys. Rev. Lett.* **70**, 1895–1899 (1993).
6. M. Żukowski, A. Zeilinger, M. A. Horne, A. K. Ekert, "Event-ready-detectors" Bell experiment via entanglement swapping. *Phys. Rev. Lett.* **71**, 4287–4290 (1993).
7. C. Branciard, N. Gisin, S. Pironio, Characterizing the nonlocal correlations created via entanglement swapping. *Phys. Rev. Lett.* **104**, 170401 (2010).
8. C. Branciard, D. Rosset, N. Gisin, S. Pironio, Bilocal versus nonbilocal correlations in entanglement-swapping experiments. *Phys. Rev. A* **85**, 032119 (2012).
9. J. F. Clauser, M. A. Horne, A. Shimony, R. A. Holt, Proposed experiment to test local hidden-variable theories. *Phys. Rev. Lett.* **23**, 880–884 (1969).
10. J.-W. Pan, D. Bouwmeester, H. Weinfurter, A. Zeilinger, Experimental entanglement swapping: Entangling photons that never interacted. *Phys. Rev. Lett.* **80**, 3891–3894 (1998).

Downloaded from http://advances.sciencemag.org/ on May 25, 2021

11. J. B. Altepeter, E. R. Jeffrey, P. G. Kwiat, Phase-compensated ultra-bright source of entangled photons. *Opt. Express* **13**, 8951–8959 (2005).
12. T. Symul, S. M. Assad, P. K. Lam, Real time demonstration of high bitrate quantum random number generation with coherent laser light. *Appl. Phys. Lett.* **98**, 231103 (2011).
13. K. Mattle, H. Weinfurter, P. G. Kwiat, A. Zeilinger, Dense coding in experimental quantum communication. *Phys. Rev. Lett.* **76**, 4656–4659 (1996).
14. N. Lütkenhaus, J. Calsamiglia, K.-A. Suominen, Bell measurements for teleportation. *Phys. Rev. A* **59**, 3295–3300 (1999).
15. P. G. Kwiat, H. Weinfurter, Embedded Bell-state analysis. *Phys. Rev. A* **58**, R2623–R2626 (1998).
16. A. G. White, A. Gilchrist, G. J. Pryde, J. L. O'Brien, M. J. Bremner, N. K. Langford, Measuring two-qubit gates. *J. Opt. Soc. Am. B* **24**, 172–183 (2007).
17. D. J. Saunders, S. J. Jones, H. M. Wiseman, G. J. Pryde, Experimental EPR-steering using Bell-local states. *Nat. Phys.* **6**, 845–849 (2010).
18. B. Hensen, H. Bernien, A. E. Dréau, A. Reiserer, N. Kalb, M. S. Blok, J. Ruitenberg, R. F. L. Vermeulen, R. N. Schouten, C. Abellán, W. Amaya, V. Pruneri, M. W. Mitchell, M. Markham, D. J. Twitchen, D. Elkouss, S. Wehner, T. H. Taminiau, R. Hanson, Loophole-free Bell inequality violation using electron spins separated by 1.3 kilometres. *Nature* **526**, 682–686 (2015).
19. M. Giustina, M. A. M. Versteegh, S. Wengerowsky, J. Handsteiner, A. Hochrainer, K. Phelan, F. Steinlechner, J. Kofler, J.-. Larsson, C. Abellán, W. Amaya, V. Pruneri, M. W. Mitchell, J. Beyer, T. Gerrits, A. E. Lita, L. K. Shalm, S. W. Nam, T. Scheidl, R. Ursin, B. Wittmann, A. Zeilinger, Significant-loophole-free test of Bell's theorem with entangled photons. *Phys. Rev. Lett.* **115**, 250401 (2015).
20. L. K. Shalm, E. Meyer-Scott, B. G. Christensen, P. Bierhorst, M. A. Wayne, M. J. Stevens, T. Gerrits, S. Glancy, D. R. Hamel, M. S. Allman, K. J. Coakley, S. D. Dyer, C. Hodge, A. E. Lita, V. B. Verma, C. Lambrocco, E. Tortorici, A. L. Migdall, Y. Zhang, D. R. Kumor, W. H. Farr, F. Marsili, M. D. Shaw, J. A. Stern, C. Abellán, W. Amaya, V. Pruneri, T. Jennewein, M. W. Mitchell, P. G. Kwiat, J. C. Bienfang, R. P. Mirin, E. Knill, S. W. Nam, A strong loophole-free test of local realism. *Phys. Rev. Lett.* **115**, 250402 (2015).
21. P. M. Pearle, Hidden-variable example based upon data rejection. *Phys. Rev. D* **2**, 1418–1425 (1970).
22. R. Kaltenbaek, R. Prevedel, M. Aspelmeyer, A. Zeilinger, High-fidelity entanglement swapping with fully independent sources. *Phys. Rev. A* **79**, 040302(R) (2009).
23. C. Erven, E. Meyer-Scott, K. Fisher, J. Lavoie, B. L. Higgins, Z. Yan, C. J. Pugh, J.-P. Bourgoin, R. Prevedel, L. K. Shalm, L. Richards, N. Gigov, R. Laflamme, G. Weihs, T. Jennewein, K. J. Resch, Experimental three-photon quantum nonlocality under strict locality conditions. *Nat. Photonics* **8**, 292–296 (2014).
24. J. S. Bell, *Speakable and Unspeakable in Quantum Mechanics* (Cambridge Univ. Press, 1989).
25. T. Fritz, Beyond Bell's theorem: Correlation scenarios. *New J. Phys.* **14**, 103001 (2012).
26. A. Tavakoli, P. Skrzypczyk, D. Cavalcanti, A. Acín, Nonlocal correlations in the star-network configuration. *Phys. Rev. A* **90**, 062109 (2014).
27. J. Hensen, R. Lal, M. F. Pusey, Theory-independent limits on correlations from generalized Bayesian networks. *New J. Phys.* **16**, 113043 (2014).
28. T. Fritz, Beyond Bell's theorem II: Scenarios with arbitrary causal structure. *Commun. Math. Phys.* **341**, 391–434 (2016).
29. C. M. Lee, R. W. Spekkens, Causal inference via algebraic geometry: Feasibility tests for functional causal structures with two binary observed variables. arXiv 1506.03880 (2015).
30. R. Chaves, Polynomial Bell inequalities. *Phys. Rev. Lett.* **116**, 010402 (2016).
31. D. Rosset, C. Branciard, T. J. Barnea, G. Pütz, N. Brunner, N. Gisin, Nonlinear Bell inequalities tailored for quantum networks. *Phys. Rev. Lett.* **116**, 010403 (2016).
32. A. Tavakoli, Bell-type inequalities for arbitrary noncyclic networks. *Phys. Rev. A* **93**, 030101 (R) (2016).
33. E. Wolfe, R. W. Spekkens, T. Fritz, The inflation technique for causal inference with latent variables. arXiv 1609.00672 (2016).
34. A. Acín, N. Brunner, N. Gisin, S. Massar, S. Pironio, V. Scarani, Device-independent security of quantum cryptography against collective attacks. *Phys. Rev. Lett.* **98**, 230501 (2007).
35. S. Pironio, A. Acín, S. Massar, A. B. de la Giroday, D. N. Matsukevich, P. Maunz, S. Olmschenk, D. Hayes, L. Luo, T. A. Manning, C. Monroe, Random numbers certified by Bell's theorem. *Nature* **464**, 1021–1024 (2010).
36. R. Colbeck, A. J. Kent, Private randomness expansion with untrusted devices. *Physica A* **44**, 095305 (2011).
37. C. Branciard, E. G. Cavalcanti, S. P. Walborn, V. Scarani, H. M. Wiseman, One-sided device-independent quantum key distribution: Security, feasibility, and the connection with steering. *Phys. Rev. A* **85**, 010301(R) (2012).
38. G. Carvacho, F. Andreoli, L. Santodonato, M. Bentivegna, R. Chaves, F. Sciarrino, Experimental non-locality in a quantum network. arXiv 1610.03327 (2016).
39. A. Fine, Hidden variables, joint probability, and the Bell inequalities. *Phys. Rev. Lett.* **48**, 291–295 (1982).
40. S. Pironio, Lifting Bell inequalities. *J. Math. Phys.* **46**, 062112 (2005).

Acknowledgments: We thank A. Abbott, N. Brunner, N. Gisin, S. Pironio, and D. Rosset for helpful discussions. **Funding:** This research was conducted by the Australian Research Council Centre of Excellence for Quantum Computation and Communication Technology (project number CE110001027). D.J.S. and C.B. acknowledge European Union Marie Curie Fellowships PIIF-GA-2013-629229 and PIIF-GA-2013-623456, respectively. C.B. acknowledges a "Retour Post-Doctorants" grant from the French National Research Agency (ANR-13-PDOC-0026). D.J.S. acknowledges support from an ERC advance grant (MOQUACINO). **Author contributions:** D.J.S., C.B., and G.J.P. conceived the experiment. D.J.S. and A.J.B. constructed and performed the experiment, with guidance from G.J.P., D.J.S., and C.B. adapted the theory to the experiment. D.J.S. performed the data analysis with help from C.B., G.J.P., and A.J.B. All authors contributed to writing the manuscript. **Competing interests:** The authors declare that they have no competing interests. **Data and materials availability:** All data needed to evaluate the conclusions in the paper are present in the paper and/or the Supplementary Materials. Additional data related to this paper may be requested from the authors.

Submitted 6 November 2016
Accepted 14 February 2017
Published 28 April 2017
10.1126/sciadv.1602743

Citation: D. J. Saunders, A. J. Bennet, C. Branciard, G. J. Pryde, Experimental demonstration of nonbilocal quantum correlations. *Sci. Adv.* **3**, e1602743 (2017).

Downloaded from http://advances.sciencemag.org/ on May 25, 2021

Science Advances

Experimental demonstration of nonbilocal quantum correlations

Dylan J. Saunders, Adam J. Bennet, Cyril Branciard and Geoff J. Pryde

Sci Adv **3** (4), e1602743.
DOI: 10.1126/sciadv.1602743

ARTICLE TOOLS http://advances.sciencemag.org/content/3/4/e1602743

SUPPLEMENTARY MATERIALS http://advances.sciencemag.org/content/suppl/2017/04/24/3.4.e1602743.DC1

REFERENCES This article cites 36 articles, 0 of which you can access for free
http://advances.sciencemag.org/content/3/4/e1602743#BIBL

PERMISSIONS http://www.sciencemag.org/help/reprints-and-permissions

Use of this article is subject to the Terms of Service

Science Advances (ISSN 2375-2548) is published by the American Association for the Advancement of Science, 1200 New York Avenue NW, Washington, DC 20005. The title *Science Advances* is a registered trademark of AAAS.

Copyright © 2017, The Authors

Downloaded from http://advances.sciencemag.org/ on May 25, 2021